

3D Modeling Visualization for Studying Controls of the Jumbo Container Crane

J.B. Klaassens, G. Honderd, A. El Azzouzi,
Ka C. Cheok,* G.E. Smid,*

Faculty of Information Technology and Systems
Control Laboratory
Delft University of Technology

Abstract

The jumbo container cranes at the European Container Terminal (ECT) in Rotterdam are subject of a long term study to automate the international seaport and make container handling more efficient. In this paper appropriate details of the 3D dynamical behavior of the container is modeled. Simulation and visualization are carried out to study the crane behavior under disturbing conditions like unbalanced center of gravity and varying side winds. The software is used to evaluate time-optimal trajectories and control schemes for the dynamics of the electrical drives, and of the swing and skew of the container.

Keywords : Container crane, 3D dynamics model, swing and skew control, gantry crane.

1 Introduction

The need for fast and safe loading and unloading container vessels whose service time is to be minimized, requires a control of the crane motion that optimizes the crane's dynamic performance. The two-dimensional cycle is divided in three motions: load hoisting, transfer and load lowering. The problems are the reduction of the total time of load transport (time-optimal trajectory control [1], [4]) and reduction of the swing of the load at its end position, including accurate positioning of the load.

During the transport of the load, the planar position is controlled by varying the position of the trolley and varying the length of the suspension rope. Specific constraints such as maximum torque (which is a maximum acceleration or deceleration of the trolley or load), maximum speed and the existance of obstacles on the quay or in the container vessel, have to be incorporated in the trajectory controller.

A validated math model is necessary for conducting detailed study of the dynamic behavior of the container crane and control schemes. Although several analyses have been made, using nonlinear models [5], [6], further increased complexity may be considered by including the detailed

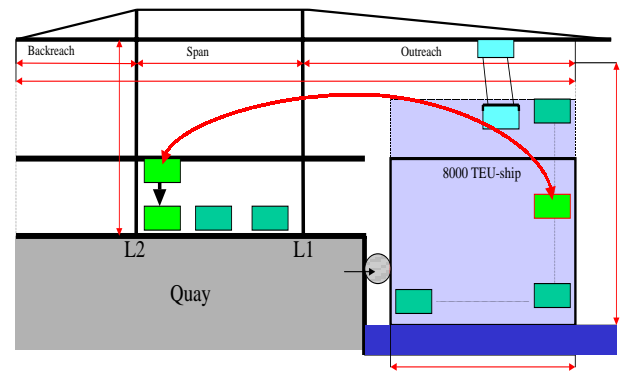


Figure 1: A schematical drawing representing loading and unloading of the Jumbo Container Crane.

construction of the crane, the stretch in the cables and the influence of wind.

A six degree of freedom (dof) model is presented in this paper to study the other modes like skew and sway. These modes will be excited by the unsymmetric characteristics of hoisting ropes, unbalanced loading of the container and the influence of wind. This model allows control schemes for the dynamical movements of the container to be studied extensively. A control concept that introduces a time-optimal trajectory [4] while minimizing the swing and the wind influence, is presented.

The structure of the paper is as follows. Section 2 presents the basic equations to obtain the 3D model of the container crane. Section 3 presents the control scheme and Section 4 shows the simulation results of the dynamic behavior of the crane.

2 Modeling

Figure 1 shows a drawing of the side elevation of the crane that is being studied in this paper. In order to model the motion dynamics of the container body, we assign two coordinate reference frames. They are the global reference frame, on the base of the rail, and the container attached reference frame, in the geometric center of the container. The

*Department of Electrical and Systems Engineering, Oakland University, Rochester MI, USA.

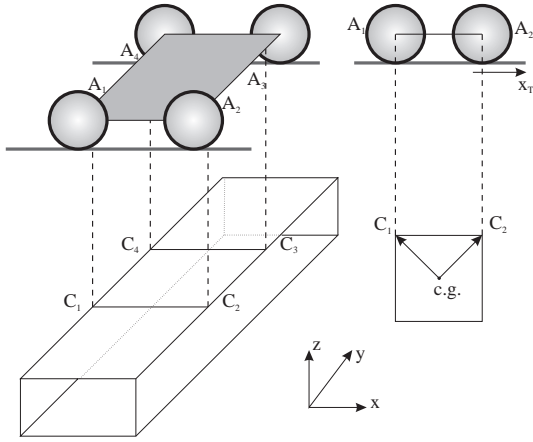


Figure 2: Geometry of trolley, container and cables.

following notation will be adopted throughout this paper

$$\text{frame } \mathbf{V}, \quad (1)$$

where \mathbf{V} is a matrix or vector. A vector with respect to the global reference frame will be denoted with ${}^o\mathbf{V}$, and with respect to the container reference frame with ${}^c\mathbf{V}$. Furthermore, matrices will be printed in bold, and vectors with overbar.

The transformation from the global reference frame to the container frame is defined by ${}^o\mathbf{R}_C$, [2] as

$${}^o\mathbf{R}_C = \mathbf{R}_x \mathbf{R}_y \mathbf{R}_z \quad (2)$$

where

$$\mathbf{R}_z = \begin{bmatrix} \cos(\psi) & \sin(\psi) & 0 \\ -\sin(\psi) & \cos(\psi) & 0 \\ 0 & 0 & 1 \end{bmatrix} \quad (3)$$

$$\mathbf{R}_y = \begin{bmatrix} \cos(\theta) & 0 & \sin(\theta) \\ 0 & 1 & 0 \\ -\sin(\theta) & 0 & \cos(\theta) \end{bmatrix} \quad (4)$$

$$\mathbf{R}_x = \begin{bmatrix} 1 & 0 & 0 \\ 0 & \cos(\phi) & \sin(\phi) \\ 0 & -\sin(\phi) & \cos(\phi) \end{bmatrix}. \quad (5)$$

where ϕ , θ and ψ are the Euler angles representing roll, pitch and yaw of the container.

2.1 Container Dynamics

Figure 2 shows the configuration of the trolley and container system. It is clear from Figure 2, that the displacement vectors for the cables can be stated as

$${}^o\bar{D}_i = {}^o\bar{A}_i - {}^o\bar{C}_i \quad \text{for } i = 1 \dots 4 \quad (6)$$

The locations of the pulleys ${}^o\bar{A}_i$ on the trolley can be derived from the trolley position on the rail x_T and the geometric design of the crane. The locations of the pulleys ${}^o\bar{C}_i$ on the container are derived from the motion of the container:

$${}^o\bar{C}_i = \bar{x} + {}^o\mathbf{R}_C {}^c\bar{C}_i \quad (7)$$

The forces in the cables are given by

$${}^o\bar{F}_i = \frac{{}^o\bar{D}_i}{|D_i|} \left(K_s S_i + K_d \dot{S}_i \right) \quad (8)$$

where K_s is the stiffness and K_d the damping coefficient, and S_i is the stretch, computed as

$$S_i = |D_i| - L_i. \quad (9)$$

Here, L_i is the unloaded length of cable i . The total force acting on the container and the spreader is the sum of cable forces ${}^o\bar{F}_i$, together with the wind force ${}^o\bar{W}$ and the gravitational force $M {}^o\bar{G}$, where M is the mass matrix. The acceleration vector of the C.G. of the container thus becomes

$${}^o\bar{a} = M^{-1} \left({}^o\bar{W} + \sum_i {}^o\bar{F}_i \right) + {}^o\bar{G}. \quad (10)$$

Since velocity and position can be found by integration of acceleration, the dynamic equations for the container mass can be represented in the diagram in Figure 3,

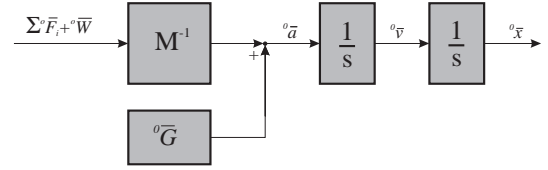


Figure 3: Model for container translational motion dynamics

A state space model description for the translational container motion can be expressed as

$$\frac{d}{dt} \begin{bmatrix} {}^o\bar{v} \\ {}^o\bar{x} \end{bmatrix} = \begin{bmatrix} 0 & 0 \\ \mathbf{I} & 0 \end{bmatrix} \begin{bmatrix} {}^o\bar{v} \\ {}^o\bar{x} \end{bmatrix} + \begin{bmatrix} M^{-1} (\sum {}^o\bar{F}_i + {}^o\bar{W}) + G \\ 0 \end{bmatrix} \quad (11)$$

The sum of the torques acting on the container and spreader can be computed by

$${}^o\bar{T} = \sum_{i=1}^4 ({}^o\bar{C}_i - {}^o\bar{x}) \times {}^o\bar{F}_i + {}^o\bar{x}_w \times {}^o\bar{W}. \quad (12)$$

where \times denoted a cross-product operation. Taking the centrifugal and coriolis acceleration into account, the instantaneous angular accelerations with reference to the container frame can be derived as

$${}^c\dot{\bar{\Omega}} = \bar{I}^{-1} \left({}^o\mathbf{R}_C^T {}^o\bar{T} - ({}^c\bar{\Omega} \times (\bar{I} \cdot {}^c\bar{\Omega})) \right). \quad (13)$$

The container gyroscopic angle rate ${}^c\bar{\Omega}$ can be found by integration. In order to find the rotation angles of the container, ${}^c\bar{\Omega}$ needs to be translated to Euler angle rates ${}^o\dot{\bar{\Theta}}$. With \vec{i} , \vec{j} and \vec{k} being the unit vectors in the x , y and z -directions respectively, the transformation

$$\mathbf{R}_f = \mathbf{R}_z \mathbf{R}_y \mathbf{R}_x \vec{i} + \mathbf{R}_z \mathbf{R}_y \vec{j} + \mathbf{R}_z \vec{k} \quad (14)$$

provides the relation

$${}^o\dot{\Theta} = \mathbf{R}_f {}^c\bar{\Omega}. \quad (15)$$

The body rotation angles ϕ , θ and ψ can be found by integration of the above equation, as the elements of ${}^o\Theta$. The diagram in Figure 4 represents the model for the angular dynamics.

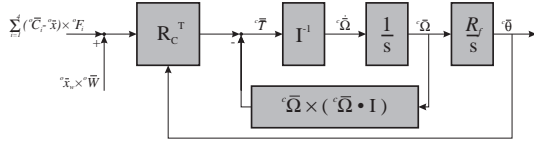


Figure 4: Model for the angular dynamics

The coriolis and centrifugal torques can be expressed in a matrix product as follows

$$\mathbf{S} \mathbf{I} {}^c\bar{\Omega} = {}^c\bar{\Omega} \times (\mathbf{I} \cdot {}^c\bar{\Omega}) \quad (16)$$

where \mathbf{S} is given by

$$\mathbf{S} = \begin{bmatrix} 0 & -\omega_z & \omega_y \\ \omega_z & 0 & -\omega_x \\ -\omega_y & \omega_x & 0 \end{bmatrix}. \quad (17)$$

The state space formulation for the angular dynamics is given by:

$$\frac{d}{dt} \begin{bmatrix} {}^c\bar{\Omega} \\ {}^o\bar{\Theta} \end{bmatrix} = \begin{bmatrix} -\mathbf{I}^{-1}\mathbf{S}\mathbf{I} & 0 \\ \mathbf{R}_f & 0 \end{bmatrix} \begin{bmatrix} {}^c\bar{\Omega} \\ {}^o\bar{\Theta} \end{bmatrix} + \begin{bmatrix} \mathbf{I}^{-1}\mathbf{R}_C \\ 0 \end{bmatrix} {}^o\mathbf{T} \quad (18)$$

2.2 Hoist, Trolley and Skew Drives

Hoist Drive. The hoisting system is configured with four 350 kW DC motors that are mechanically connected to the drum shaft through a gear box. The gearbox is configured to optimize the power-speed ratio of the system.

In order to control the force in the hoisting cables the armature currents of the motors are controlled. This requires an extra feedback of the motor currents. The drive system model is graphically represented in the diagram in Figure 5.

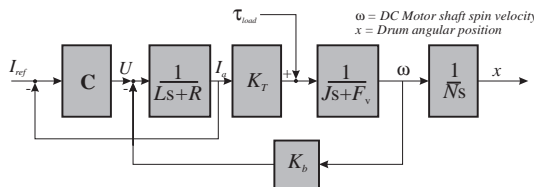


Figure 5: A typical linear model for the DC Drive and Motor systems

When a PI-controller is considered for the current controller C ,

$$C(s) = K_P + K_I \frac{1}{s}, \quad (19)$$

then the drive control system can be represented in state space form as

$$\frac{d}{dt} \begin{bmatrix} U_i \\ I_a \\ \omega \\ x \end{bmatrix} = \begin{bmatrix} 0 & -K_i & 0 & 0 \\ \frac{1}{L} & \frac{-K_p + R}{L} & \frac{-K_b}{L} & 0 \\ 0 & \frac{K_T}{J} & \frac{F_v}{J} & 0 \\ 0 & 0 & \frac{1}{N} & 0 \end{bmatrix} \begin{bmatrix} U_i \\ I_a \\ \omega \\ x \end{bmatrix} + \begin{bmatrix} K_I \\ \frac{K_P}{L} \\ 0 \\ 0 \end{bmatrix} \begin{bmatrix} I_{ref} \\ \tau_{load} \end{bmatrix} \quad (20)$$

In this formulation, U_i stands for the control output of the integral part of the PI-current controller and I_{ref} is the reference current command. The load torque τ_{load} on the hoist drive shaft, caused by the force in the cables, is modeled as

$$\tau_{load} = \frac{d_\tau}{N} \sum_i {}^o\bar{F}_i. \quad (21)$$

Trolley drive. The control and dynamics model for the hoisting drive system does also apply to the DC machine that drives the trolley system. However, the feedback load torque for the trolley system is the horizontal component of the forces in the cables,

$$\tau_{load} = \frac{d_\tau}{N} \sin(\eta) \sum_i {}^o\bar{F}_i \quad (22)$$

where η is the swing angle.

Skew drive. The skew drive system consists of a motor actuation that can shift one side (two cables) of the hoist mechanism on the trolley forward and backward so that the cables apply a yaw torque on the container and spreader. Again, the similar model of the DC-drive and motor system can be applied to describe the skew control drive.

2.3 State Space Formulation

The objective for the space container crane system modeling is to derive a parameterized input-output formulation, that will predict motions and forces of the container and the trolley, for a given trajectory \mathcal{R} and a given set of electric drive controllers C_T , C_H and C_S (The controller design schemes will be discussed in the following section).

From this perspective, Equations (6), (8) and (12) can be used to express the inputs of the systems (11), (18) and (20) as functions of each others states. Only for the input currents to the DC drives we need the expression for the controller models as functions of the system states.

As shown in Figure 6, the control strategy consists of a trajectory planner and a set of controllers (C_T , C_H and C_S) for controlling the motion of the container. In this paper we will present only some examples of the simple controllers that have been used to illustrate the simulation and visualization aspects of the crane project.

We remarked the several extensive studies such as time optimal control [4], model predictive control [3], etc, that have been conducted and will be reported in the future.

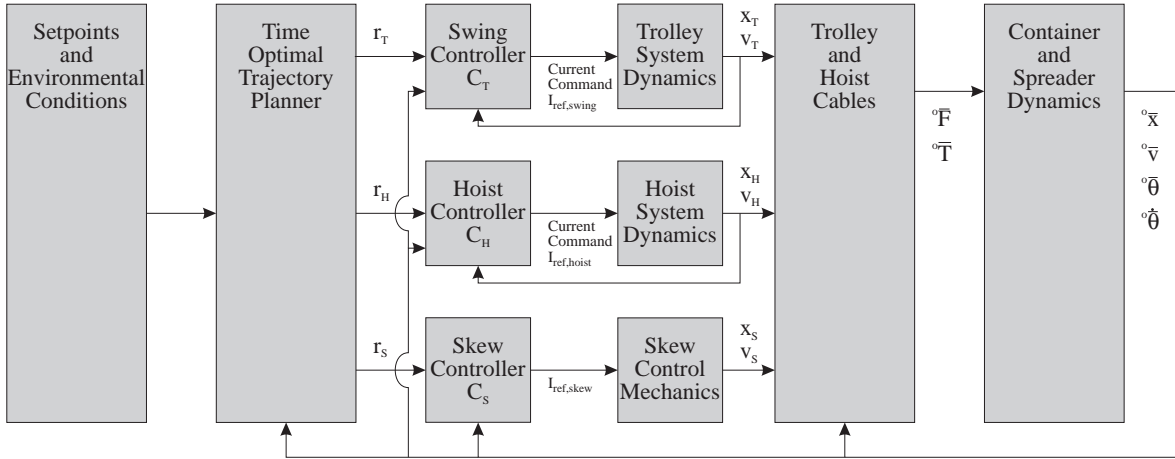


Figure 6: Overview of the control strategy for the Container Crane System.

3 Control

An important objective of the automated container crane system is to regulate the swing motion of the container. The criterion for controller design for transferring a container from the ship to the shore concerns with the time of travel that begins when the spreader locks onto a container and which ends as soon as the container hangs just above its end location with an error of less than 5 cm.

For this purpose a time-optimal trajectory is planned (details can be found in [4]) and used as a reference path for the container to follow. The control strategy therefore is to “drive” the container along the time-optimal path in the quickest manner while minimizing the swing and skew in the motion.

3.1 Swing Control

The horizontal container position can be expressed as

$$x_C = x_T + \left(\hat{L}_i + \frac{1}{2}h_C \right) \sin(\eta) \quad (23)$$

which is the trolley position plus the offset of the container caused by swing. h_C denotes the height of the container and \hat{L}_i is the actual length of the cables when they are stretched. In the control scheme, x_C is subtracted from the reference input for container position x_R . Furthermore, the trolley speed \dot{x}_T , swing angle η and swing velocity $\dot{\eta}$ are fed back. The swing dynamics are sensed with a CCD camera.

For our illustration, the swing controller C_T is defined by

$$C_T : \quad I_{ref,swing} = K_{T,swing}[x_{ref,T} - x_C - K_{T,\dot{x}}\dot{x}_T + K_{T,\eta}\eta - K_{T,\dot{\eta}}\dot{\eta}] \quad (24)$$

3.2 Skew Control

Skew is the name for the angular motion about the vertical axis of the container. It is measured using two CCD cameras. It occurs when, for example, the left and right cables are not

equal in length. Once the swing period for the left and right side of the container will be different. Additionally, skew can be caused by side wind as well as unbalanced loading in the container.

Several methods exist for controlling skew motion. The two methods of interest are

- Independent control of the left and right hoisting cable lengths, which will effectively change the swing time of the left and right hoisting cables;
- Shifting of the left or right pulley’s along the x -direction of the trolley, which will effectively apply an additional skew torque as damping on the disturbance skew motion.

The latter method is used in the simulation described in this paper. The pulley positions on the trolley on the left rail are given by

$$\bar{A}_i(x) = \bar{A}_{i+2}(x) + \Delta_S \quad \text{for } i = 1, 2 \quad (25)$$

where Δ_S represents the pulley positions difference between the left and the right side of the trolley. For our illustration, the skew controller is implemented as a damper, i.e.

$$C_S : \quad I_{ref,skew} = K_S \dot{\psi}. \quad (26)$$

where $\dot{\psi}$ is the skew rate.

3.3 Hoist Control

Similarly, the hoist control is implemented as a P-controller,

$$C_H : \quad I_{ref,hoist} = K_H(L_{ref} - \hat{L}_i). \quad (27)$$

4 Simulation & Animation

Figure 7 shows the signals for trolley position, container position and swing angle in a simulation of the container for moving from the center to the left and to the far right in the work plane. Also a 3D animation of the crane has been developed.

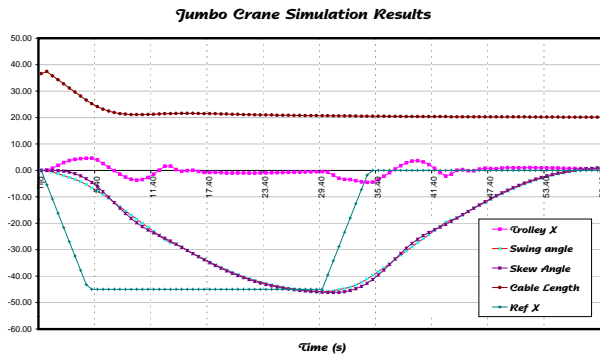


Figure 7: Simulation output results of trolley and container position x_T and swing angle η as a function of time.

5 Conclusions

The 3-D math model for the dynamics of hoisting a container with the JCC 2000 Jumbo Container Crane has been presented. The drives and the control schemes have been discussed.

Simulation results with a simple controller to stabilize the swing and the skew of the container have shown satisfying and promising results.

The modeling and the controller design for the Jumbo Container Crane is a big and involved task. For example, the time-optimal control must not only move the container quickly to its destination, but also do this within the numerous constraints for currents torques and speeds, but also within a positioning accuracy of 5 cm.

Other more sophisticated control solutions will follow in future papers.

References

- [1] J. W. Auernig and H. Troger. Time optimal control of overhead cranes with hoisting of the load. *Automatica*, 23(4):437–447, 1987.
- [2] A. Craig. *Introduction to Robotics*. Addison Wesley, 3rd edition, 1996.
- [3] Peter J. Van der Veen. Trajectregelaar voor containerkranen (i). Master's thesis, Delft University of Technology, 1998.
- [4] P. Hippe. Time optimal control of an overhead crane. *Regeltechnik und Prozess-Daten arbeitung*, 18(8):346–350, 1970.
- [5] A. J. Ridout. Anti swing control of the overhead crane using linear feedback. *Journal of Electrical and Electronic Engineering*, pages 17–26, 1989.

- [6] Y. Sakawa and Y. Shindo. Optimal control of container cranes. *Automatica*, 18(3):257–266, 1982.
- [7] D.T. Greenwood. *Principles of Dynamics*, Prentice Hall, Englewood Cliffs, NJ, 1965.
- [8] G.E. Smid, Ka C. Cheok and T.K. Tan, Multi-CPU real-time simulation of vehicle systems. Proceedings of the 7th International Conference on Intelligens Systems (ICIS '98) Melun Fontainebleau, France July 1-2 1998.
- [9] G.E. Smid, Ka C. Cheok and K. Kobayashi, Modeling of Vehicle Dynamics using Matrix-Vector Oriented calculations in Matlab. Proceedings of the ISCA 9th International Conference on Computer Applications in Industry and Engineering (CAINE), Orlando, FL, Dec 11-13, 1996.
- [10] K. Kobayashi, K. Watanabe, Ka C. Cheok and G.E. Smid, S Simple Vehicle Dynamics Modeling usig Object Oriented Approach. *Japan Journal of Instrumentation and Control Engineering*, Jan 7, 1997.
- [11] C. Burhenne, G. Honderd and J.B. Klaassens, Modeling the non-linearities and non-stiffness of a Jumbo Container Crane. *Technical report, Control Lab, Faculty of Information Technology and Systems, Delft University of Technology*. Delft, the Netherlands, June 29, 1998.